packings tested, it is probably unfair to make a precise comparison with perforated plates. Further research probably will show certain packings in the proper column diameter: packing diameter ratio to be as good or better than perforated or bubble cap plates.

When 1,5-pentanediol is the extractive distillation agent, the perforated plate column gives a separation of an apparent relative volatility of ethyl acetate to ethanol of 3.19. With helices it is 2.32; with Berl saddles, 2.08; with Intalox saddles, 2.02; and with Raschig rings, 2.08. These data show that, although packed columns may not be quite as efficient as perforated plate columns, they can indeed be used in extractive distillation.

LITERATURE CITED

Berg, L., "Separation of Ethylbenzene from p- and m-Xylene by Extractive Distillation," U.S. Patent 4,292,142 (Sept. 29, 1981).

Drout, Jr., W. M., and J. W. Dowling, "Process to Dehydrate Alcohols Using Glycols," Fr. Patent 1,020,351 (Nov. 19, 1952).

Schneible, J., "Dehydration of Ethanol Using Glycerol," U.S. Patent 1,469,447 (Oct. 2, 1923).

Smith, P. V., and C. S. Carlson, "Dehydration of Ethanol with Ethoxyethanol or Butoxyethanol," U.S. Patent 2,559,519 (July 3, 1951).

Manuscript received November 8, 1982; revision received February 8, and accepted March 16, 1983.

Catalytic Conversion of Large Molecules: Effect of Pore Size and Concentration

D. D. DO

Department of Chemical Engineering
University of Queensland
St. Lucia, Qld. 4067, Australia

INTRODUCTION

Catalytic conversion of large molecules, such as heavy petroleum residue and coal-derived liquids, involves the restricted pore-diffusion transport of such molecules into the catalyst pellets. The sizes of molecules in these feedstocks range between 25×10^{-10} m and 150×10^{-10} m. The largest fraction is around 50×10^{-10} m (Ruckenstein and Tsai, 1981).

The degree of restriction of these molecules by the pore wall has been the subject of many investigations (Colton et al., 1975; Prasher and Ma, 1977; Prasher et al., 1978).

The catalytic conversion of large molecules, optimal pore size of catalyst pellets, has been reported for heavy petroleum residue (Eigenson et al., 1977; Ohtsuka, 1977) and for coal-derived liquids (Brooks et al., 1976; and Yet et al., 1976). In this paper we shall investigate the optimal pore size for these feedstocks with the assumption of first-order chemical kinetics (Sapre et al., 1980; Schuit and Gates, 1973). The interaction between diffusing molecules and the surface may play an important role in catalytic conversion of large molecules. In fact, Glandt (1981) has shown that the concentration is higher in the periphery of the pore than at the center. This interaction, however, is ignored in this work because the emphasis of this paper is on the interplay among diffusion, reaction and the nonlinear partition coefficient. Such interaction could be incorporated, but the mathematical analysis would then be very difficult.

SINGLE CATALYST PELLET

The mass balance equation for the reactant in the catalyst pellet is

$$D_e \frac{1}{r^2}\frac{\partial}{\partial r}\left(r^2 \frac{\partial C}{\partial r}\right) - \rho_p S_g k'' C = 0, \tag{1}$$

where

$$D_e = \frac{\epsilon_p D_b}{\tau} K_r. \tag{2}$$

The drag coefficient K_r, proposed by Renkin (1954) in his study of porous cellulose membrane, is used here in our analysis

$$K_r = 1 - 2.104\lambda + 2.09\lambda^3 - 0.95\lambda^5, \tag{3}$$

where

$$\lambda = a/r_p \tag{4}$$

The surface area is related to the pore radius and the pore volume as follows

$$r_p = 2V_g/S_g \tag{5}$$

We shall assume that the pore volume does not change with the pore radius. Thus, the surface area is proportional to the inverse of the pore radius.

Substituting Eq. 2 into Eq. 1, we obtain:

$$\frac{\epsilon_p D_b}{\tau} K_r(\lambda) \frac{1}{r^2}\frac{d}{dr}\left(r^2 \frac{dC}{dr}\right) - \rho_p k'' \frac{S_{go} r_{po}}{r_p} \cdot C = 0. \tag{6}$$

At the pellet center, the usual symmetry condition

$$r = 0; \quad dC/dr = 0. \tag{7}$$

At the surface of the catalyst pellet, due to the comparable dimension between the rectangular molecular size and the pore size, partition coefficient was often used in many works. However, in the recent work of Glandt (1981), the pore surface concentration is nonlinearly related to the bulk concentration as follows:

$$C(R) = C_b\left[K_o + K_1^*\left(\frac{C_b}{C_m}\right) + K_2^*\left(\frac{C_b}{C_m}\right)^2\right], \tag{8}$$

where C_b is the bulk concentration, K_o is defined as for cylindrical pore

$$K_o = (1 - \lambda)^2, \tag{9}$$

and K_1^*, K_2^* are defined numerically in Glandt (1981) as functions of λ. C_m is defined as $C_m = 1/N_A d^3$. For our subsequent analysis, we have fitted a sixth-order polynomials to the curves of K_1^* and K_2^* vs. λ and have found

$$\frac{K_1^*}{K_o} = a\lambda + b\lambda^2 + c\lambda^3 + d\lambda^4 + e\lambda^5 + f\lambda^6, \tag{10}$$

where

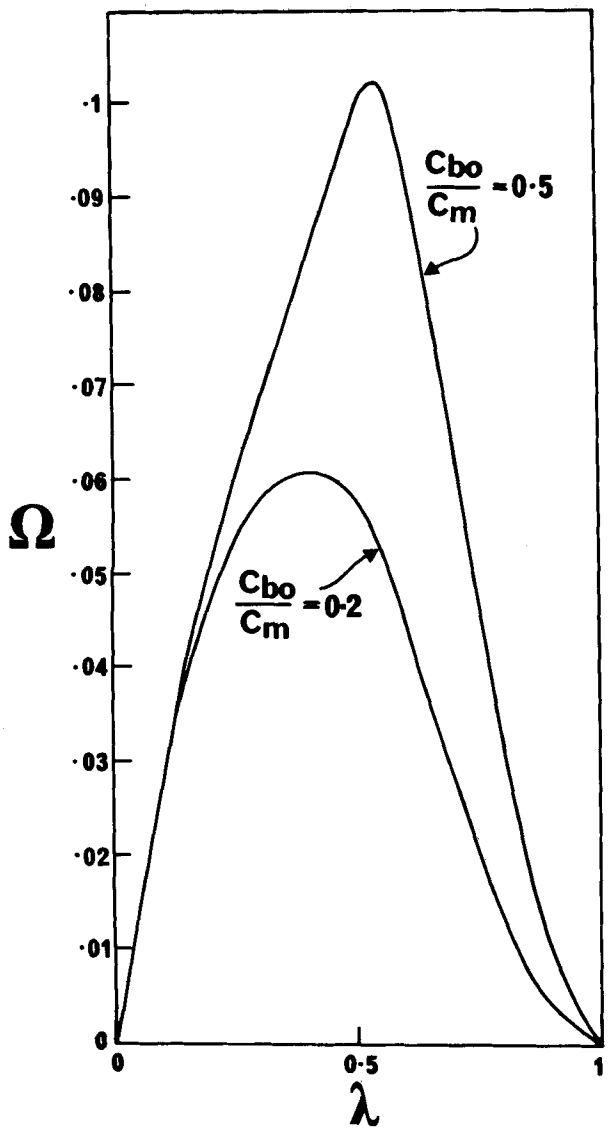

Figure 1. Plot of nondimensional reaction rate vs. reactant/pore size ratio for $\phi_o = 1$.

$$\left.\begin{aligned} a &= 3.441710 & b &= -3.818080 \\ c &= 61.419275 & d &= -226.648785 \\ e &= 426.348267 & f &= -304.456892 \end{aligned}\right\} \quad (11)$$

and

$$\frac{K_2^*}{K_o} = a'\lambda + b'\lambda^2 + c'\lambda^3 + d'\lambda^4 + e'\lambda^5 + f'\lambda^6, \quad (12)$$

with

$$\left.\begin{aligned} a' &= 2.133881 & b' &= -123.295985 \\ c' &= 1{,}007.599639 & d' &= -3{,}763.450227 \\ e' &= 6{,}551.702482 & f' &= -4{,}113.405604 \end{aligned}\right\} \quad (13)$$

By defining the following nondimensional variables and parameters

$$y = C/K_oC_b, \quad x = r/R, \quad \epsilon = C_b/C_m, \quad \phi_o^2 = \frac{R^2\rho_p k'' S_{go} r_{po}}{\epsilon_p D_b a}, \quad (14)$$

Equations 6 and 8 become:

$$\frac{1}{x^2}\frac{d}{dx}\left(x^2\frac{dy}{dx}\right) - \frac{\phi_o^2\lambda}{g(\lambda)}y = 0, \quad (15a)$$

$$x = 0; \quad dy/dx = 0, \quad (15b)$$

$$x = 1; \quad y = 1 + \frac{K_1^*}{K_o}\epsilon + \frac{K_2^*}{K_o}\epsilon^2 \quad (15c)$$

where

$$g(\lambda) = 1 - 2.104\lambda + 2.09\lambda^3 - 0.95\lambda^5. \quad (16)$$

Solution to Eqs. 15 is

$$y = \left[1 + \frac{K_1^*(\lambda)}{K_o(\lambda)}\epsilon + \frac{K_2^*(\lambda)}{K_o(\lambda)}\epsilon^2\right]\frac{\sinh\left[\phi_o\sqrt{\frac{\lambda}{g(\lambda)}}\cdot x\right]}{x\cdot\sinh\left[\phi_o\sqrt{\frac{\lambda}{g(\lambda)}}\right]} \quad (17)$$

The quantity of practical interest is the amount of chemical reaction rate inside the catalyst pellet. Its nondimensional form is

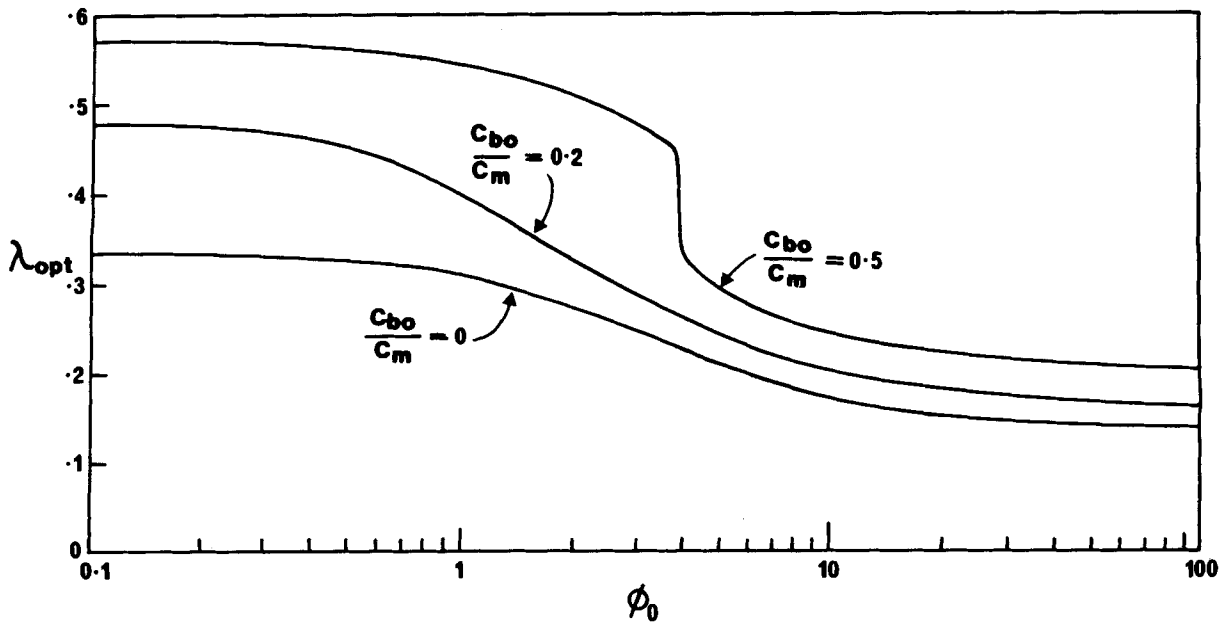

Figure 2. Optimal reactant/pore size ratio, λ_{opt}, vs. ϕ_o with bulk concentration as parameter.

$$\Omega = \frac{4\pi R^2 \mathcal{D}_e \left.\frac{\partial C}{\partial r}\right|_R}{\underline{(4\pi R \epsilon D_b C_b)}} = g(\lambda)(1-\lambda)^2 \left[1 + \frac{K_1^*(\lambda)}{K_o(\lambda)}\epsilon + \frac{K_2^*(\lambda)}{K_o(\lambda)}\epsilon^2\right]$$
$$\tau$$
$$\cdot \left\{\phi_o \sqrt{\frac{\lambda}{g(\lambda)}} \coth\left[\phi_o \sqrt{\frac{\lambda}{g(\lambda)}}\right] - 1\right\}. \quad (18)$$

The last bracket term in the RHS of Eq. 18 increases with λ, and $(1-\lambda)^2$ decreases with λ. Therefore, there exists an optimum λ such that the nondimensional reaction rate is maximum (Figure 1). The existence of this optimum pore size is due to the fact that increase in pore size has two conflicting effects. The surface area decreases and the diffusion rate increases. Therefore, the optimum pore size exists irrespective whether the partition coefficient is linear or nonlinear with respect to bulk concentration. Figure 2 shows the plots of λ_{opt} versus parameter ϕ_o with ϵ as parameter. The value of $C_{bo}/C_m = 0.5$ used corresponds to a concentration close to 30% by volume. This is probably too high for virial series treatment. Glandt (1981) in fact presented his result up to $C_{bo}/C_m = 0.4$. Therefore, extrapolation to higher C_{bo}/C_m is not recommended. Clearly, the optimum λ_{opt} is not only a function of ϕ_o but also a strong function of the bulk concentration. If the linear partition coefficient had been applied, such dependence of λ_{opt} on the bulk concentration would not have been observed. In fact, the lowest curve in Figure 2 is the curve that would have been obtained for the case of linear partition coefficient. It is interesting to observe a steep drop on λ for $C_{bo}/C_m = 0.5$. This steep drop is due to the inherent behavior of the partition coefficient K vs. λ obtained by Glandt (1981) (Figure 4 in his paper). In fact, in his Figure 4, when $C_{bo}/C_m = 0.4$ the parameter λ changes abruptly for K about 0.6.

The nonlinear partition coefficient proposed by Glandt (1981) reduces the optimal pore size. For example, when $\phi_o = 1$, $\epsilon = 0.2$, $a = 25 \times 10^{-10}$ m (typical molecular radius) of heavy petroleum residue) the optimal pore radius calculated from the nonlinear partition theory is 62.3×10^{-10} m (Figure 2, middle curve) while the optimal pore radius calculated from the linear partition theory is 80.6×10^{-10} m. Thus, the linear partition theory over-predicts the optimal pore radius by 30%. The reasons for this lower optimum pore radius is because the nonlinear partition coefficient proposed by Glandt (1981) enhances the concentration of diffusion species on the surface.

A plot of λ_{opt} vs. (C_b/C_m) with ϕ_o as parameter is shown in Figure 3. For subsequent analysis of a fixed bed reactor, we fit a parabolic polynomial to the curve of λ_{opt} vs. (C_b/C_m)

$$\lambda_{opt} = \alpha_o + \alpha_1 \left(\frac{C_b}{C_m}\right) + \alpha_2 \left(\frac{C_b}{C_m}\right)^2, \quad (19)$$

where α_o, α_1 and α_2 are functions of ϕ_o and are tabulated in Table 1. We observe the concavities of the curves change as ϕ_o increases (Figure 3). This change is due to the inherent behavior of K versus λ (Glandt, 1981, Figure 4).

FIXED BED REACTOR

Consider a fixed bed reactor containing porous catalyst pellets. The mass balance equation in the reactor is

$$u\frac{dC_b}{dz} + (1-\epsilon_b)\frac{3}{R}\mathcal{D}_e \left.\frac{\partial C}{\partial r}\right|_R = 0; \quad z = 0, \quad C_b = C_{bo} \quad (20)$$

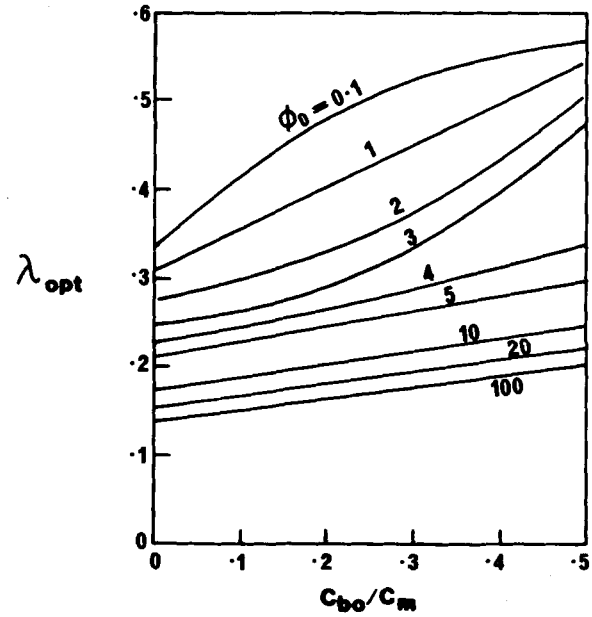

Figure 3. Optimal reactant/pore size ratio, λ_{opt}, vs. bulk concentration (C_b/C_m), with ϕ_o as parameter.

The mass balance equation inside the porous catalyst and its associated boundary conditions are given in Eqs. 6, 7 and 8. By defining the following nondimensional variables and parameters

$$y = C/K_o C_{bo}, \quad \omega = C_b/C_{bo}, \quad x = r/R, \quad \epsilon = C_{bo}/C_m, \quad (21a)$$

$$\zeta = z/L, \quad \gamma = 3(1-\epsilon_b)\epsilon \frac{\mathcal{D}_{bL}}{R^2 u \tau},$$
$$\phi_o^2 = \frac{R^2 \rho_p k'' S_{go} r_{po} \tau}{\epsilon \mathcal{D}_b a}, \quad (21b)$$

Equations 6, 7, 8 and 20 become Eqs. 15a and 15b

$$x = 1; \quad y = \omega\left[1 + \frac{K_1^*(\lambda)}{K_o(\lambda)}\epsilon\omega + \frac{K_2^*(\lambda)}{K_o(\lambda)}\epsilon^2\omega^2\right], \quad (22)$$

$$\frac{d\omega}{d\zeta} + \gamma g(\lambda) K_o(\lambda) \left.\frac{\partial y}{\partial x}\right|_1 = 0; \quad \zeta = 0, \quad \omega = 1, \quad (23)$$

respectively.

For optimal operation of the fixed bed reactor, the parameter λ_{opt} must be related to the bulk concentration as in Eq. 19. In terms of ω, it is

$$\lambda_{opt} = \alpha_o + \alpha_1 \epsilon\omega + \alpha_2 \epsilon^2 \omega^2. \quad (24)$$

Solution to Eqs. 15a, 15b, 22 and 23 is

$$\frac{d\omega}{d\zeta} = \gamma F(\omega, \lambda)$$

where

$$F(\omega,\lambda) = -g(\lambda)K_o(\lambda)\omega\left[1 + \frac{K_1^*(\lambda)}{K_o(\lambda)}\epsilon\omega + \frac{K_2^*(\lambda)}{K_o(\lambda)}\epsilon^2\omega^2\right]$$
$$\cdot\left\{\phi_o\sqrt{\frac{\lambda}{g(\lambda)}}\coth\left[\phi_o\sqrt{\frac{\lambda}{g(\lambda)}}\right] - 1\right\}. \quad (26)$$

TABLE 1. CONSTANTS α_1, α_2 AND α_3 AS FUNCTIONS OF ϕ_o

ϕ_o	0.1	1	2	3	4	5	10	20	100
α_0	0.3320	0.3100	0.2750	0.2470	0.2270	0.211	0.1740	0.1540	0.1390
α_1	0.8923	0.4477	0.1407	0.0447	0.1520	0.170	0.1483	0.1367	0.1243
α_2	−0.8367	0.0367	0.6467	0.8267	0.1400	0.	−0.0167	−0.0033	0.0033

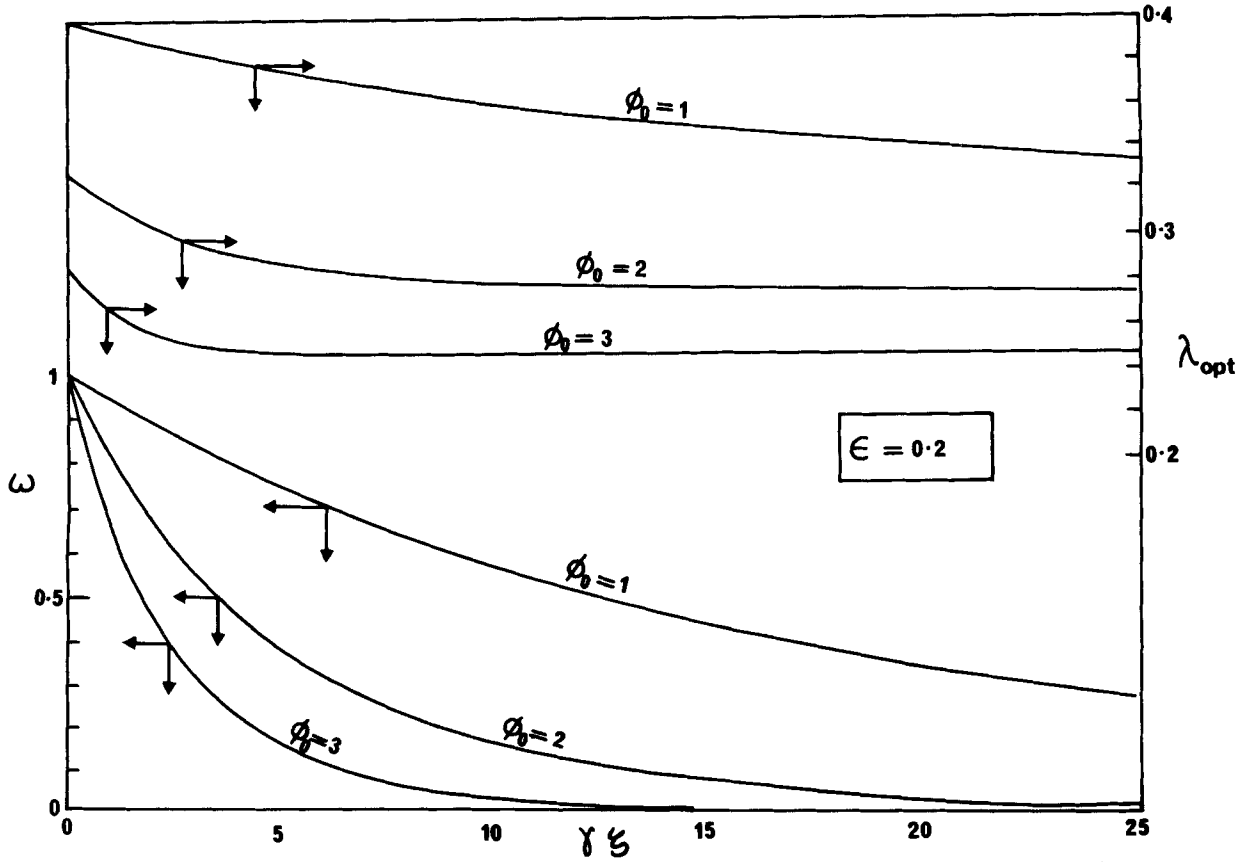

Figure 4. Plot of reactant concentration and optimal reactant/pore size ratio λ_{opt} vs. reactor length for $\epsilon = 0.2$ and $\phi_o = 1, 2, 3$.

Since λ is algebraically related to ω was in Eqs. 24, Eq. 25 can be rewritten:

$$\frac{d\omega}{d\zeta} = \gamma G(\omega) \underset{\equiv}{def} \gamma F(\omega, \lambda(\omega)). \tag{27}$$

Solution to Eq. 17 can be written in terms of quadrature

$$\int_1^{\omega} \frac{d\omega}{G(\omega)} = \gamma \cdot \zeta \tag{28}$$

Knowing ω as a function of ζ, λ as a function of ζ can be obtained directly from Eq. 24. This function will give the optimal pore radius distribution for a given reactant molecular size.

Figure 4 shows the concentration and the optimal pore radius vs. the nondimensional distance ζ for $\epsilon = 0.2$ and various values of ϕ_o. As expected from the previous section result on single pellet studies, the optimum λ_{opt} decreases as the bulk concentration decreases. To illustrate the advantage of the optimal profile, we calculate the reduced length for the case of $\epsilon = 0.5$, $\phi_o = 1$. For such a case, the reduced length $\gamma\zeta$ for 90% conversion is 38 for the optimal reactor. For the same set of parameter, if the pore size distribution is uniform throughout the reactor and is equal to the optimal pore size at the entrance, the reduce length $\gamma\zeta$ for 90% conversion is 46. Thus the optimal reactor cuts down the length by 17%.

The optimum pore size is seen to be a continuous function of reactor axial distance. Although it would be difficult to produce catalysts with varying pore size, it is still feasible that certain pore size catalysts could be packed in one section, other pore size catalysts could be packed in other section of the reactor and so on, depending on the availability of different pore size catalyst commercially.

CONCLUSION

The determination of optimal pore size for the catalytic conversion of large molecules, such as heavy petroleum residue or coal-derived liquid, in a single catalyst pellet has been presented in this paper. The optimal pore size not only depends on the physico-chemical characteristic of the reacting system but also on the bulk concentration surrounding the catalyst pellet. The fixed bed reactor containing such catalysts has also been analyzed theoretically, and it was found that for running the reactor in an optimal fashion, the pore size must be a function of distance along the reactor. In fact, for a given reactant molecular size, the pore size must increase along the reactor to compensate for the depletion of the reactant concentration.

NOTATION

a	= reactant molecular radius
C	= intraparticle concentration
C_b	= bulk concentration
C_m	= concentration, $(=1/N_A d^3)$
d	= molecular size
D_e	= effective diffusivity
F	= function, defined in Eq. 26
g	= function defined in Eq. 16
k''	= surface reaction constant
K_r	= drag coefficient
K_o	= linear partition coefficient defined in Eq. 9
K_1^*, K_2^*	= coefficients defined in Eq. 8
N_A	= Avocadro number
r	= radial coordinate
r_p	= pore radius
r_{po}	= reference pore radius
S_g	= interior surface area per unit mass
S_{go}	= reference interior surface area per unit mass
u	= superficial fluid velocity
V_g	= pore volume per unit mass
x	= nondimensional radial coordinate
y	= nondimensional intraparticle concentration

Greek Letters

α_j = coefficients defined in Eq. 24
γ = parameter defined in Eq. 21
ϵ = parameter defined in Eq. 14
ϵ_b = bed voidage
ϵ_p = pellet voidage
λ = ratio of reactant molecular size to pore size
ρ_p = pellet density
τ = tortuosity factor
ϕ_o = parameter defined in Eq. 14
Ω = nondimensional reaction rate defined in Eq. 18
ζ = nondimensional distance along the reactor

LITERATURE CITED

Brooks, J. A., R. J. Bertolacini, L. C. Gutberlet, and D. K. Kim, "Catalyst Development For Coal Liquefaction," EPRI Publication AF-190, Electric Power Research Institute, Palo Alto (1976).

Colton, C. K., C. N. Satterfield, and C. Lai, "Diffusion and Partitioning of Macromolecules Within Finely Porous Glass," *AIChE J.* **21**, 289 (1975).

Eigenson, A. S., et al., "An Effective Catalyst for the Hydrodesulphurization of Heavy Petroleum Stocks," *Int. Chem. Eng.*, **17**, 332 (1977).

Glandt, E. D., "Distribution Equilibrium between a Bulk Phase and Small Pores," *AIChE J.*, **27**, 51 (1981).

Ohtsuka, T., "Catalyst for Hydrodesulphurization of Petroleum Residue," *Cat. Rev. Sci. Eng.*, **16**, 291 (1977).

Prasher, B. D., and Y. H. Ma, "Liquid Diffusion in Microporous Alumina Pellets," *AIChE J.*, **23**, 303 (1977).

Prasher, B. D., G. A. Gabriel, and Y. H. Ma, "Restricted Diffusion of Liquids in Microporous Catalysts," *AIChE J.*, **24**, 1118 (1978).

Renkin, E. M., "Filtration, Diffusion, and Molecular Sieving Through Porous Cellulose Membranes," *J. Gen. Physiol.*, **28**, 225 (1954).

Ruckenstein, E., and M. S. Tsai, "Optimum Pore Size For the Catalytic Conversion of Large Molecules," *AIChE J.*, **27**, 697 (1981).

Sapre, A. V., et al., "Hydrodesulphurization of Benzo[b]naptho[2,3,-d] thiophene Catalyzed by Sulfide CoO-MoO_3/γ-Al_2O_3: The Reaction Network," *AIChE J.*, **26**, 690 (1980).

Schuit, G. C. A., and . C. Gates, "Chemistry and Engineering of Catalytic Hydrodesulphurization," *AIChE J.*, **19**, 417 (1973).

Yen, Y. K., D. E. Furlani, and S. W. Weller, "Batch Autoclave Studies of Catalytic Hydrodesulphurization of Coal," *Ind. Eng. Chem. Proc. Res. Dev.*, **15**, 24 (1976).

Manuscript received March 2, 1983; revision received May 19, and accepted May 31, 1983.

Decomposition Strategy for the Synthesis of Minimum-Unit Heat Exchanger Networks

DANIEL MOCSNY and RAKESH GOVIND

Department of Chemical and Nuclear Engineering
University of Cincinnati
Cincinnati, OH 45221

INTRODUCTION

The heat exchanger network synthesis problem has been reviewed by Nishida et al. (1981). We consider the problem with n_h hot streams and n_c cold streams, each with given flow rate, heat capacity, inlet and target temperatures. We adopt the terminology and notation of Flower and Linnhoff (1980) and Nishida et al. (1981).

In previous work, the "minimum number" of heaters, coolers, and exchangers required to solve the problem, n_{min}, is given as one less than the total number of streams and services (Hohmann, 1971):

$$n_{min} = n_h + n_{hs} + n_c + n_{cs} - 1 \tag{1}$$

where

n_{cs} = number of hot services

n_{hs} = number of cold services

Flower and Linnhoff note that when heat recovery demands are stringent, i.e., when heat is to be transferred between streams across a small temperature difference, the minimum number of exchangers may be larger than this. Flower and Linnhoff also note that occasionally a solution may be produced which exhibits fewer units than this "minimum" number, and they give an example solution for 10SP1 exhibiting only nine units. In this work the conditions under which such solutions can be produced are explored, and a strategy for locating them efficiently is proposed.

Linnhoff et al. (1979) illustrate the manner in which the number of heat exchanger units in a solution can be reduced by dividing the problem into two separate components. In this work such a strategy is adopted and applied to a problem of unprecedented size and is found to yield desirable benefits from a design and operability standpoint.

ADVANTAGES OF THIS METHOD

The Decomposition Strategy yields these benefits:

1) Solutions are produced containing fewer heat exchangers for a given problem than would be expected based on Eq. 1.

2) Very large reductions in computational difficulty are realized, facilitating the solution of large problems with 20 streams or more.

3) Actual designs based on the resulting solutions exhibit modularity and independent operation, simplifying controllability.

ESTABLISHING THE MINIMUM NUMBER OF EXCHANGERS

If we ignore the heat loads, temperature compatibilities, etc., of the hot and cold streams, leaving only the requirement that every stream be matched at least once, the minimum number of exchangers required is only as large as the larger of the set of hot

Correspondence concerning this paper should be addressed to R. Govind.